PERGAMON

Aerosol Science 34 (2003) 1445–1463

Journal of
Aerosol Science

www.elsevier.com/locate/jaerosci

Absorption of light by soot particles: determination of the absorption coefficient by means of aethalometers

E. Weingartner[a,*], H. Saathoff[b], M. Schnaiter[b], N. Streit[a], B. Bitnar[c], U. Baltensperger[a]

[a] *Laboratory of Atmospheric Chemistry, Paul Scherrer Institut, Villigen CH-5232, Switzerland*
[b] *Laboratory for Micro- and Nanotechnology, Paul Scherrer Institut, Villigen CH-5232, Switzerland*
[c] *Institute of Meteorology and Climate Research, Forschungszentrum Karlsruhe, D-76021 Karlsruhe, Germany*

Received 25 November 2002; accepted 14 May 2003

Abstract

During a soot aerosol measurement campaign the response of two different aethalometers (AE10 with white light and AE30 with multiwavelength capability) to several types of soot was investigated. Diesel soot, spark-generated carbon particles, and mixtures of these soot particles with ammonium sulfate and oxidation products of α-pinene were used in this evaluation. The determination of the particles light absorption coefficient (b_{abs}) with the AE10 aethalometer is a difficult task because of an ill-defined spectral sensitivity of this instrument. Provided that the proper numerical corrections are performed, the AE30 instrument allows for the measurement of b_{abs} over a wide spectral range ($\lambda = 450$–950 nm). During all experiments it was found that with increasing filter load the optical path in the aethalometer filter decreased. As a result, an increased underestimation of the measured aethalometer signals (b_{abs} or black carbon mass concentrations) occurs with increasing filter loads. This effect, which is attributed to a "shadowing" of the particles in the fiber matrix, is very pronounced for "pure" soot particles while almost negligible for aged atmospheric aerosols. An empirical correction for this bias is presented and requires information on the light scattering behavior (i.e. light scattering coefficient) of the sampled particles. Without this additional information, the applicability of the instruments is limited. Comparison with a reference method shows that multiple scattering in the nearly unloaded fiber filter is responsible for enhanced light absorption by a factor of about 2.14.

Keywords: Absorption coefficient; Black carbon; Light attenuation; Aethalometer calibration; Multiple scattering; Single scattering albedo

* Corresponding author. Tel.: +41-56-310-2405; fax: +41-56-310-4525.
E-mail address: ernest.weingartner@psi.ch (E. Weingartner).

0021-8502/$ - see front matter © 2003 Elsevier Ltd. All rights reserved.
doi:10.1016/S0021-8502(03)00359-8

1. Introduction

Carbon is one of the most abundant constituents of ambient particulate matter and is either present as organic carbon (OC), which is mainly volatile and/or reactive in a heated air stream, or as elemental carbon (EC), which is non-volatile and non-reactive, or as carbonate. The characterization of carbonaceous particles is a very active field, especially with respect to its effects on human health and atmospheric radiative properties, and interaction with clouds.

Mainly due to the presence of EC, ambient particulate material appears black when collected on a filter. Therefore, black carbon (BC) is defined as the fraction of carbonaceous aerosol absorbing light over a broad region of the visible spectrum, and is measured by determining the attenuation of light transmitted through the sample. Among all available optical absorption or light attenuation methods, the aethalometer, as described by Hansen, Rosen, and Novakov (1984), is the most frequently used technique to measure *real-time* BC mass concentrations. The classic aethalometers (AE9 and AE10, MAGEE Scientific; Berkeley, USA) work with an incandescent lamp and broadband detectors. Hundreds of these instruments are installed worldwide, and some have been in continuous operation for over a decade. In the last years, new aethalometers and light attenuation instruments have been developed operating with several light sources with narrow bandwidths ranging from the near ultraviolet to the near infrared.

In this paper, we present and discuss optical measurements performed during an extensive soot aerosol campaign in the AIDA aerosol chamber of the Research Center Karlsruhe in October 1999. During this campaign, artificially generated soot, Diesel engine soot, ammonium sulfate $(NH_4)_2SO_4$ particles, and mixtures of the above components were characterized as a function of aging time. In order to simulate atmospheric aging processes, soot particles were coated with organic material from the ozonolysis of α-pinene. The aim of this paper is to present correction factors for the use of the aethalometer.

2. Theory

2.1. Beer–Lambert's law

The absorption coefficient (b_{abs}) is defined with Beer–Lambert's law

$$I = I_0 \, e^{-b_{abs} \cdot x}, \tag{1}$$

where I_0 is the intensity of the incoming light and I the remaining light intensity after passing through a medium with the thickness x. The attenuation (ATN) is typically given as percentage values and is defined by the relationship

$$\mathrm{ATN} \equiv \ln\left(\frac{I_0}{I}\right). \tag{2}$$

Aethalometers measure the light attenuation through a quartz filter matrix where the fiber filter is assumed to act as a perfect diffuse scattering matrix in which the light-absorbing particles are embedded. Two detectors monitor the light transmission through the filter; one measures the light passing through the particle-laden sample spot while the other measures the light passing through a

particle-free reference part of the filter. This is done to correct for variations in incident light intensity and drift in electronics. According to the Beer–Lambert's law (Eq. (1)), the aerosol absorption coefficient of the filtered aerosol particles b_{ATN} (henceforth referred to as the attenuation coefficient) is defined as

$$b_{\mathrm{ATN}} \equiv \frac{A}{Q}\frac{\Delta \mathrm{ATN}}{\Delta t}, \tag{3}$$

where A is the filter spot area, Q the volumetric flow rate and ΔATN is the change in attenuation during the time interval Δt.

2.2. Empirical model

It is well known that b_{ATN} may differ significantly from the true aerosol absorption coefficient b_{abs} of airborne particles. Therefore, the calibration factors C and $R(\mathrm{ATN})$ are introduced, which can be used to convert aethalometer attenuation measurements to "real" absorption coefficients:

$$b_{\mathrm{abs}} = b_{\mathrm{ATN}}\frac{1}{C \cdot R(\mathrm{ATN})}, \tag{4}$$

where C and R describe the two effects which change the optical properties of filter embedded particles with respect to the properties of the same particles in the airborne state. The first effect is responsible for C being greater than unity and is caused by multiple scattering of the light beam at the filter fibers in the unloaded filter. This leads to an enhancement of the optical path and thus to enhanced light absorption of the deposited particles (Liousse, Cachier, & Jennings, 1993). This effect is illustrated in Ballach, Hitzenberger, Schultz, and Jaeschke (2001) who demonstrated that these scattering effects can be minimized by immersion of the particle loaded filters in oil with a refracting index similar to the filter fibres. The empirical constant C mainly depends on the nature of the filter and the apparatus used. Any other effects that are caused by deposited particles are described by the empirical function $R(\mathrm{ATN})$ which varies with (a) the amount of aerosol particles embedded in the filter and (b) optical properties of the deposited particles. For unloaded filters R is set to unity, i.e. $R(\mathrm{ATN} = 0) = 1$. With the gradual increase in attenuation due to the accumulating particles in the filter the absorbing particles in the filter absorb a higher fraction of the scattered light which leads to a reduction of the optical path in the filter ($R < 1$). As a consequence, generally lower attenuation coefficients are measured for higher filter loadings than for lightly loaded filters. In the following this effect is named shadowing effect. One has to mention that this term is a somewhat misleading description as submicrometer particles do not visibly cast shadows. If light scattering particles are embedded in the filter matrix, the shadowing effect may be partially reduced and R may exhibit a smaller decrease with increasing loading of the filter. This phenomenon is due to additional light scattering arising from the transparent aerosol material. R will thus also depend on the single scattering albedo ω_0 of the sampled aerosol, which is defined as

$$\omega_0 \equiv \frac{b_{\mathrm{s}}}{b_{\mathrm{e}}} = \frac{b_{\mathrm{s}}}{b_{\mathrm{abs}} + b_{\mathrm{s}}}, \tag{5}$$

where b_{s} and b_{e} are the aerosol light scattering and extinction coefficients, respectively.

For the derivation of b_{abs}, the exact knowledge of the empirical calibration values C and R is of great importance. C was determined for aethalometers operating with incandescent lamps and was

found to be approximately 1.9–2.5 (see Petzold, Kopp, & Niessner, 1997 and references therein). Bodhaine (1995) used this relation with $C = 1.9$ to calculate b_{abs} from aethalometer measurements performed during several years at different stations in Alaska, Hawaii, and Antarctica. It has to be noted that in these studies the C values were derived under the assumption that R is equal to unity over the measured ATN range, which is typically 0–50%.

So far, the influence of the filter loading, i.e., the function $R(\mathrm{ATN})$ was rarely investigated. A lot of studies rely on Gundel, Dod, Rosen, and Novakov (1984) who found that the BC mass loading of aethalometer filters is linearly related to their ATN, which means that R is equal to unity. This is in contrast to newer findings. Lindberg, Douglass, and Garvey (1999) have shown with a radiative transfer model that this linear relationship is only valid for thin aerosol layers with a high fraction of black carbon. LaRosa, Buckley, and Wallace (2002) operated two aethalometers in parallel inside a house located in an urban environment and found that the instrument with the higher filter loading gave lower readings than the other until the instruments tape advance, where a filter change caused an apparent increase of ~50%. In that study a correction method was developed that reduced the error of this bias by a factor of 2. A distinct $R < 1$ dependence is also applied in the processing of the ATN data obtained from the particle soot/absorption photometer (PSAP, Radiance Research) (Reid et al., 1998). The working principle of the PSAP is similar to the aethalometer. The light transmission is also continuously measured through a quartz fiber substrate at a wavelength λ of 550 nm but the PSAP does not perform automatic filter changes. For the b_{abs} calculation the PSAP algorithm uses the following empirical corrections:

$$C = 1.79 \text{ and } R = 0.4 + 0.6\exp(-\mathrm{ATN}/100\%). \tag{6}$$

In a calibration work (Bond, Anderson, & Campbell, 1999) it was found that (a) this correction still overestimates the true absorption coefficient by about 20–30% and (b) that the apparent PSAP light absorption measurement must be accompanied by a light scattering measurement to provide a scattering correction. In this context one has to mention that a comparison of the PSAP and aethalometer correction functions is difficult because different filter tapes are used in these instruments.

2.3. Calculation of the BC concentration

The exact knowledge of these empirical correction factors is also of great importance if the attenuation data is converted to BC mass loadings. The aerosol black carbon mass concentration M_{BC} (in units of g m^{-3}) is related to the absorption and attenuation coefficients by

$$M_{BC} = \frac{b_{abs}}{\sigma_{abs}} = \frac{b_{ATN}}{\sigma_{ATN} \cdot R(\mathrm{ATN})}, \tag{7}$$

where σ_{abs} and $\sigma_{ATN} \equiv \sigma_{abs} \cdot C$ are the mass specific absorption and attenuation cross-sections (in units of m^2 g^{-1}), respectively. σ_{ATN} strongly depends on the aerosol type and age (Liousse et al., 1993; Petzold & Niessner, 1995). The observed variability in σ_{ATN} (measured with the incandescent lamp instrument) ranges from 5 m^2 g^{-1} (remote areas) to 9.3 m^2 g^{-1} at a remote continental site (Lavanchy, Gäggeler, Nyeki, & Baltensperger, 1999) to 14 m^2 g^{-1} at urban locations and to 20 m^2 g^{-1} at near-street measuring sites (Liousse et al., 1993). Measurements with spark discharge generated ultrafine BC test aerosol yielded σ_{ATN} values of 3.2–4 m^2 g^{-1} (Petzold & Niessner, 1995). Care has to be taken when applying these values because the reliability of the reference thermal and

solvent methods is still being debated. A comparison study (Schmid et al., 2001) showed that results from different EC determination methods are highly variable and range over more than one order of magnitude. A fraction of the variability in σ_{ATN} has therefore to be attributed to the different reference procedures applied.

Another problem arises from the fact that all the above reported σ_{ATN} values were determined under the assumption that the BC content of the filter is proportional to the measured light attenuation, i.e., these calibration studies assumed that $R(ATN)$ is equal to unity. As will be shown below this assumption is not always valid which means that these σ_{ATN} values were predominately underestimated. As will be shown below, this underestimation is pronounced for freshly emitted soot particles and almost negligible for aged atmospheric aerosols.

In the companion paper (Saathoff et al., 2003c) the aethalometer BC measurements obtained during this AIDA campaign are compared with other carbon mass determination techniques. For this comparison we used the "raw" BC values as they are directly delivered by the aethalometer data acquisition software. This means that the BC concentrations were calculated with the assumption $R = 1$ and with the σ_{ATN} values recommended by the manufacturer. These values are 19 $m^2\ g^{-1}$ for the AE10 aethalometer operating with the incandescent lamp and $\sigma_{ATN} = 14625\ nm\ m^2\ g^{-1}\lambda^{-1}$ for the AE30 instrument. During all experiments it was found that the raw aethalometer signals decreased with increasing particle load of the filter. Therefore, for this comparison study we calculated average BC values by interpolating the raw values to the mean filter light attenuation of 35% and 25% for the AE30 and AE10, respectively.

For the determination of the AE30 BC concentration only the measurement at near infrared channel at $\lambda = 880$ nm was used. It is a common practice to use this specific wavelength for BC measurement because it allows the best comparability with the AE10 instrument. Another reason for this choice is that lower wavelengths have stronger contributions by compounds other than BC. The attenuation cross-sections of other substances like hematite (Fe_2O_3) and certain organics such as aromatics rise significantly with decreasing wavelength in the near ultraviolet or even in the visible region (Lindberg, Douglass, & Garvey, 1993). This fact is why most soil and rural airborne dust samples have a brownish color. Since not all organics have UV absorbance, and the aromatics have widely varying absorption efficiencies, the UV channels cannot be used for a quantitative determination of mass concentrations. Nevertheless, the presence of strong UV absorption is an indicator for the presence of Fe_2O_3 or some organic compounds.

3. Experimental

All AIDA chamber experiments were carried out under atmospheric conditions (~40% relative humidity, 296 K) on time scales of 1–3 days. Model soot particles (in the following referred to as Palas soot particles) were generated by using two graphite spark generators (GfG 1000, Palas) and directly introduced into the aerosol chamber. Diesel soot was generated with a commercial turbo Diesel engine (VW, TDI, 1.9 l) working at 2500 rpm with a load of 17 kW. At the end of the exhaust pipe of the engine the aerosol was diluted 1:10 with synthetic air and sent through three denuders in series to reduce the water, hydrocarbon, and NO_x concentrations before the aerosol entered the chamber. The $(NH_4)_2SO_4$ aerosol was generated using an ultrasonic nebulizer (Sinaptec, GA 2400) and diffusion dryers. Organic coatings were prepared by first admixing ozone to the

aerosol in the chamber, followed by the addition of α-pinene. Details about the experiments are found in the introduction paper (Saathoff, Möhler, Schurath, Kamm, & Dippel, 2003a).

The light absorption of filtered aerosol particles was determined by means of two different aethalometers. One instrument (AE10, MAGEE Scientific; Berkeley, USA) is operated with an incandescent lamp with a broadband spectral distribution. The spectral response of this instrument is insufficiently characterized in literature. Therefore, we decided to disassemble the AE10 and to measure: (i) the emission spectrum of the lamp, (ii) the spectral transmittance of the optical components and (iii) the spectral sensitivity of the detectors (i.e. the silicon photodiodes). The lamp spectrum was measured with an Acton Research SP-300i spectrometer, which was calibrated with an integrating sphere calibration lamp. A Perkin Elmer lambda 19 spectrometer was used to determine the transmittance spectrum. The photodetector sensitivity was accessed using a spectral response setup for solar cells, which consists of an Oriel Cornerstone 130 monochromator and a calibrated powermeter. Fig. 1a shows the measured emission radiation power P of the incandescent lamp. The maximum intensity is clearly located in the infrared, and the measured intensity distribution can be well described by black body radiation at $T = 2300$ K. This lamp is mounted at the top of an optical

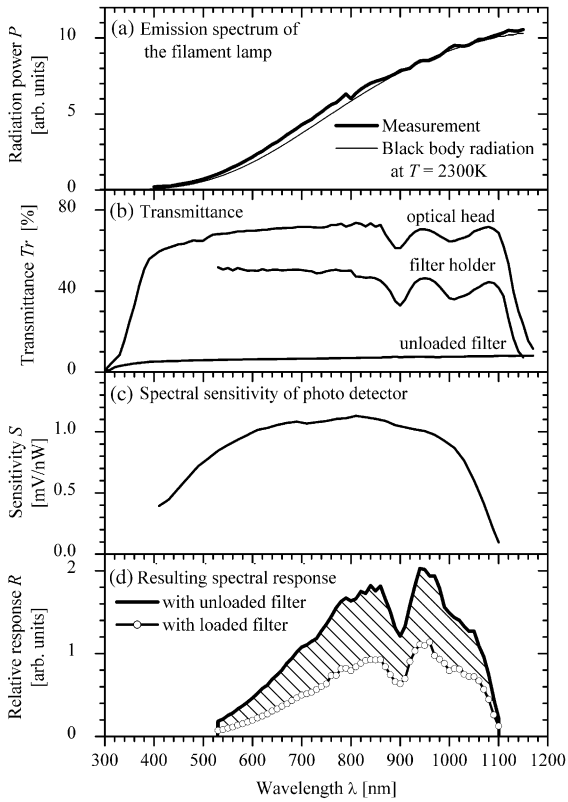

Fig. 1. Measured radiation power P of the filament bulb (a) and the transmittance Tr of the optical components of the AE10 aethalometer (b). Together with the spectral sensitivity S of the photo detector (c) the spectral response R (d) of this instrument was calculated with an unloaded and particle loaded filter (see text).

head, which is made of Lucite (acrylic plastic) and is surrounded by a metal reflector. The output of the lamp first passes through the optical head, then through the aerosol-collecting quartz fiber filter, and finally through a filter holder, which is also partially made of Lucite. Fig. 1b shows the measured light transmittance Tr of these components. Fig. 1c shows the measured spectral sensitivity S of the photo detectors (ratio of detector output voltage to the incoming light power). From these measurements the relative response $R = P \cdot Tr \cdot S$ of the AE10 aethalometer was calculated (Fig. 1d). For a setup with a particle free filter this spectral response is characterized by a broad band centered at $\lambda = 855$ nm. The distinct minimum at λ=900 nm is due to the absorption of the Lucite material. Fig. 1d also shows the spectral sensitivity of the AE10 instrument operating with a loaded filter. For this calculation, we measured the transmittance of a loaded aethalometer filter (not shown in Fig. 1c) that had sampled "pure" Diesel soot particles during an AIDA experiment.

For the calculation of b_{ATN} the aethalometer uses the difference of light transmission through the particle laden sample spot and a particle-free part of the filter. Since the AE10 instrument integrates over the whole spectral range, the shaded area in Fig. 1d, which is the difference between the spectral response of the unloaded and loaded filter, represents the final spectral response of the instrument. This shaded area is centered at $\lambda = 840$ nm which is lower than the center determined for the unloaded filter only. This difference is due to the wavelength-dependent absorption of the filtered particles. Since the wavelength dependence of b_{ATN} may change with the aerosol type, a precise assignment of the measured attenuation coefficient to a certain wavelength is not possible for the AE10 instrument.

In addition to the AE10, a prototype of the spectrum aethalometer (AE30) was also operated during the campaign. This instrument measures the light attenuation with different solid-state light sources at $\lambda = 450$, 590, 615, 660, 880, and 950 nm. According to the manufacturer, the emission spectra of each of these sources have a typical half-width of 20 nm. The attenuation at 571 nm was also measured but is not included into the further data evaluation because of ill-defined emission spectra of the corresponding diode. The main difference between the prototype employed in this study and the commercially available instruments (AE31) is that the newer instruments are operated with other solid-state light sources (i.e. $\lambda = 370$, 470, 550, 590, 660, 880, and 950 nm).

The two aethalometers were operated with different filter media. The AE-10 employed a binder free quartz filter tape from Pallflex© (type: 2500QAT-UP). This filter allows for a further qualitative EC analysis with a reference method. The AE30 instrument was operated with a quartz filter tape from the same company (type: Q250F) which has an added support layer of a non-woven polyester. The difference in tensile strength between the two products is quite apparent.

The volumetric airflow rate through each instrument was set to $5\ \mathrm{l\ min^{-1}}$ and was checked periodically (every second day) with a bubble flow meter. The instruments were connected to the same sampling line, which was periodically switched with pinch valves between filtered room air and the aerosol sampled from the AIDA aerosol chamber. This was done to minimize dilution of the aerosol in the chamber due to the relatively high flow rates of the aethalometers. Both aethalometers were operated with a time resolution of 2 min.

The reference absorption coefficient b_{abs} for airborne particles was determined by simultaneously measuring the extinction and scattering coefficient, b_e and b_s, and was obtained by $b_{abs} = b_e - b_s$. This method works well for strongly absorbing aerosols, since the difference $b_e - b_s$ is large. For small absorption the subtraction leads to large uncertainties, but still yields useful data. b_e was measured with a flow tube extinction spectrometer ($\lambda = 230$–1000 nm) and a folded path extinction

cell ($\lambda = 473$ nm), and b_s was obtained with a three-color integrating nephelometer (TSI 5660, at $\lambda = 450$, 550, and 700 nm). The truncation error of the nephelometer, which is due an angular integration restricted to 7–170°, was estimated from scattering calculations. A systematic error of the order of 5–10% in the scattering coefficient was accounted for in the estimation of the absorption coefficient error. The experimental setup and technical details concerning these devices are described in Schnaiter et al. (2003). In this paper, the spectrum aethalometer data at $\lambda = 450$ and 660 nm are compared with the temporarily measured reference absorption and scattering coefficients. Since no in situ measurements of b_s at $\lambda = 660$ nm were available, the data at $\lambda = 550$ and 700 nm were interpolated to $\lambda = 660$ nm with the Ångström power law $b = \text{constant}\ \lambda^{-\alpha}$. The Ångström exponent α of b_{abs} and b_s for Diesel and Palas soot aerosols were taken from Schnaiter et al. (2003) and are not repeated here.

4. Results and discussion

4.1. Aethalometer response to non-absorbing aerosol particles

In some experiments the optical properties of "pure" $(NH_4)_2SO_4$ particles (exp no. 4, see Saathoff et al. (2003a) for experiment numbers), particles produced by ozonolysis of α-pinene (exp no. 10) as well as $(NH_4)_2SO_4$ particles coated with oxidation products of α-pinene (exp no. 8) were investigated. During these experiments the extinction and scattering coefficient of the airborne particles, b_{ext} and b_s, were nearly identical, and thus no significant absorption coefficient b_{abs} could be calculated. Therefore, for these experiments the attenuation coefficient b_{ATN} derived from the aethalometer is compared with the scattering coefficient of the airborne particles. Table 1 shows 40-min averages (and standard deviations) of b_{ATN} (derived from the spectrum aethalometer at three different wavelengths) and values of b_s (derived from the nephelometer) for different non-absorbing aerosols. It can clearly be seen that the aethalometer showed a noisy, but clear response to the non-absorbing particles, i.e. ratios of $b_{ATN}/b_s = 0.7 \pm 0.2\%$ were typically found for $(NH_4)_2SO_4$ particles (exp no. 4). Typically, higher ratios ($b_{ATN}/b_s = 1$–5%) were measured for particles produced by ozonolysis of α-pinene

Table 1
Attenuation coefficients b_{ATN} measured with the spectrum aethalometer for non-absorbing aerosols, i.e. "pure" $(NH_4)_2SO_4$ particles (exp no. 4), particles produced by ozonolysis of α-pinene (exp no. 10) as well as a mixture of both (exp no. 8)

		Spectrum aethalometer b_{ATN}			Nephelometer b_s	
Exp no.	Aging time (h)	$\lambda = 450$ nm (m^{-1})	$\lambda = 660$ nm (m^{-1})	$\lambda = 880$ nm (m^{-1})	$\lambda = 450$ nm (m^{-1})	$\lambda = 660$ nm (m^{-1})
4	22	2.6 ± 0.2 E−5	1.8 ± 0.4 E−5	1.1 ± 0.2 E−5	3.9 ± 0.3 E−3	2.4 ± 0.1 E−3
10	13.6	1.9 ± 2.6 E−6	2.9 ± 3.6 E−6	2.4 ± 3.3 E−6	1.7 ± 0.1 E−4	6.0 ± 0.3 E−5
8	13.2	1.1 ± 0.3 E−5	9.0 ± 3.8 E−6	6.8 ± 2.0 E−6	2.6 ± 0.2 E−3	1.9 ± 0.1 E−3

The scattering coefficients b_s from the nephelometer are added for comparison and the value at $\lambda = 660$ nm was interpolated from adjacent wavelengths.

indicating that the refractive index of these compounds has a higher imaginary part than the one of $(NH_4)_2SO_4$.

The aethalometer response to "pure" $(NH_4)_2SO_4$ particles is lower than the one determined for the PSAP: Bond et al. (1999) found that in this instrument about 2% of the light scattered by the $(NH_4)_2SO_4$ particles is interpreted as absorption. To what extent the different filter materials or the size of the test aerosol particles are responsible for this difference remains an open question. In addition, impurities of absorbing material in the scattering material may render such measurements and such a comparison difficult. Penaloza (2000) determined a ratio of $b_{abs}/b_s = 2\%$ for airborne $(NH_4)_2SO_4$ particles using a cell transmissometer and partially attributed this absorption to a contamination problem.

Altogether, the measured instrumental response of the aethalometer to purely scattering aerosols is relatively small (b_{ATN}/b_s is typically smaller than a few percent). The situation is different for mixed aerosol particles. As will be shown below, the non-absorbing particles will gain in influence when they are deposited together with light absorbing material in the filter. In this case the non-absorbing particles scatter more light toward the absorbing particles resulting in an enhanced apparent absorption. On the other hand, the absorbing particles in the filter absorb a higher fraction of the scattered light which leads to a reduction of the optical path in the filter (shadowing effect). These two effects are counteracting. For all investigated aerosol types (pure soot particles, the various mixed aerosols as well as the aged aerosol at the high alpine site) we found that the shadowing effect only partially compensates the enhanced light scattering effect. The influence of non-absorbing particles is clearly seen in a reduction of the shadowing effect (lower f-values, see below).

4.2. Aethalometer response to soot particles

In the following the different processes influencing the aethalometer response to light absorbing particles are exemplified with an experiment where artificial soot particles were coated with secondary organic material (exp no. 9). Details about this experiment are found in Saathoff et al. (2003b). Briefly, at the experimental time $t = -2$ h the AIDA chamber was filled with Palas soot particles. At $t = -16$ min O_3 was injected with a final concentration of ~ 500 ppb in the chamber. At $t = 0$ approximately 61 ppb α-pinene was added and the subsequent ozonolysis of α-pinene led to a coating of the Palas soot particles. As an example, Fig. 2 shows the temporal evolution of the spectrum aethalometer data at $\lambda = 450$ nm as well as the reference light absorption and scattering data of the airborne particles for this experiment. It is clearly seen in Fig. 2a that the ATN measured with the aethalometer increases continuously until ATN$= \sim 95\%$ is reached. At this ATN a filter change is performed and after a waiting time of ~ 5 min, the measurement continues with an ATN of $\sim 10\%$. During this experiment, the spectrum aethalometer performed a total of 19 filters changes. Constant ATN values were measured during times where the instruments sampling line was switched to filtered room air. Fig. 2b shows b_{ATN}, which was calculated with Eq. (3). It is clearly seen that b_{ATN} is strongly dependent on the loading of the filter: With increasing attenuation, lower b_{ATN} values are measured indicating that R decreases with increasing filter load. This artefact, which we attribute to the shadowing effect, will be discussed in more detail in Section 4.2.1.

The intermittently measured scattering coefficient b_s (at $\lambda = 450$ nm) and the reference absorption b_{abs} are included in Fig. 2c for comparison. Here, b_{abs} was calculated with the extinction cell

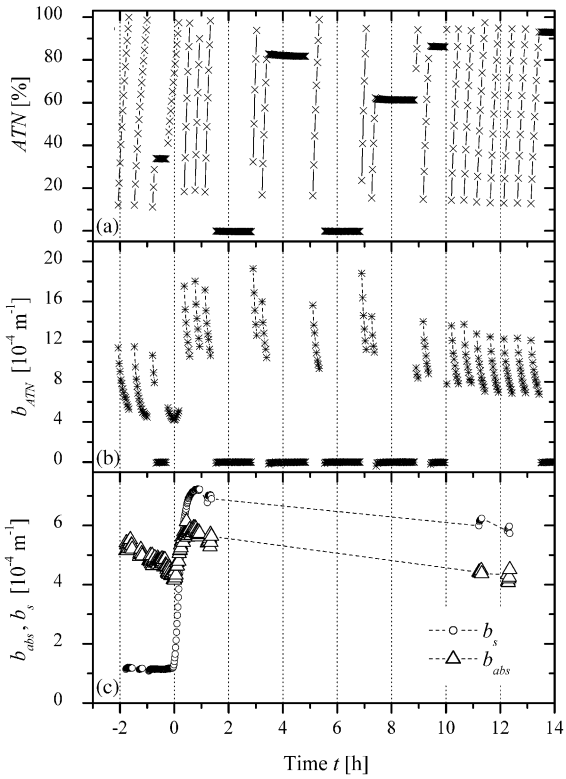

Fig. 2. Temporal evolution of measured optical parameters during experiment 9, where Palas soot particles were coated with oxidation products of α-pinene at $t = 0$. Attenuation (a) was measured with the spectrum aethalometer at $\lambda = 450$ nm, from which the attenuation coefficient b_{ATN} (b) was deduced. Constant ATN were measured when the instrument was connected to particle free air. The corresponding measurement of the reference absorption b_{abs} (at $\lambda = 475$ nm) and scattering coefficients b_{s} (interpolated to $\lambda = 475$ nm) for airborne particles are also shown (c) (Schnaiter et al., 2003). The decrease of b_{abs} and b_{s} in the time periods $-2\ \mathrm{h} < t < 0\ \mathrm{h}$ and $1\ \mathrm{h} < t < 13\ \mathrm{h}$ are due to dilution as well as sedimentational and diffusional losses.

measurement (at $\lambda = 473$ nm) and with b_{s} interpolated to the same wavelength (473 nm). Due to the multiple scattering in the fiber matrix the aethalometer measures typically 2–4 times higher attenuation coefficients than the reference method. It is also clearly seen that the coating of the soot particles with transparent material at $t = 0$ leads to a significant increase in b_{abs} as also described in Schnaiter et al. (2003). This result is explained by the encapsulation of the Palas soot particles with transparent material, which leads to an increase in the absorption cross-section. Despite the shadowing effect, the overall trend of b_{ATN} in Fig. 2b shows a similar increase at $t = 0$ and this enhancement is more pronounced for filtered than for airborne particles: Within 1 h after onset of the coating, b_{abs} and b_{ATN} show an increase of about 35% and 100%, respectively. A similar distinct enhancement in absorption was observed in an experiment where Diesel soot particles were coated with oxidation products of α-pinene. A detailed analysis of this phenomenon is presented in Section 4.2.2.

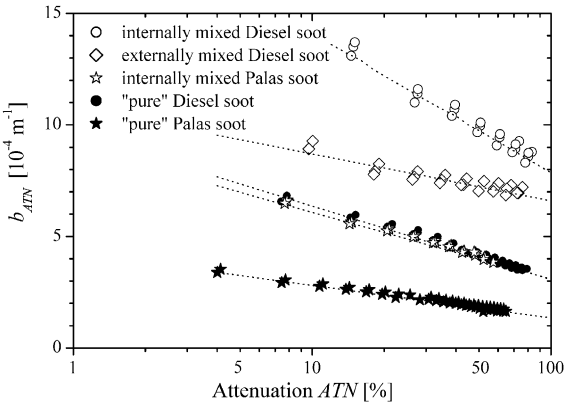

Fig. 3. Measured AE10 aethalometer signals (symbols) as a function of ATN for different aerosols. An empirical curve (dotted lines) was fitted to the data (Eq. (8), see text) which allows a parameterization of the observed shadowing effect.

4.2.1. Parameterization of the shadowing effect

The dependency of b_{ATN} on ATN can be quantified during time periods where the aerosol concentration is sufficiently constant over the time period necessary to perform more than one filter change. For such conditions, Fig. 3 shows measured attenuation coefficients as a function of ATN for different internal and external mixtures of scattering material with Diesel or Palas soot particles. As already seen in Fig. 2, generally lower attenuation coefficients are measured with increasing ATN. The data presented in Fig. 3 was obtained with the AE10 instrument, but the same distinct tendency was also observed in all channels of the AE30 instrument (see below). In order to quantify this shadowing effect and to make a comparison of the different experiments possible, the following linear empirical curve was fitted to the data

$$b_{\mathrm{ATN}} = b_{10\%}\ R(\mathrm{ATN})$$

with

$$R(\mathrm{ATN}) = \left(\frac{1}{f} - 1\right) \frac{\ln(\mathrm{ATN}) - \ln(10\%)}{\ln(50\%) - \ln(10\%)} + 1 \tag{8}$$

where $b_{10\%}$ is the value of b_{ATN} interpolated to ATN = 10% and f is a measure for the slope of the curve. $R(\mathrm{ATN})$ in Eq. (8) is a linear function of ln(ATN) and the form of this equation was chosen such that the only free parameter f can easily be interpreted. The f values allow estimating the instrumental error which occurs when the shadowing effect is disregarded. For example, $f = 1.5$ means that an ATN change from 10% to 50% leads to a reduction in b_{ATN} by $(f-1)/f \cong 33\%$.

During time periods where the sampled aerosol concentration was sufficiently constant (typically < 1 h), the aethalometer data was parameterized with this empirical curve, and the fit parameters f and $b_{10\%}$ were determined as a function of aging time. The deduced values of fit parameter f are given in Table 2 for all experiments, and the fitted curves are also included in Fig. 3, showing that the empirical curve fits the data very well.

In Table 2 data are also reported for ambient aerosols, i.e. $R(\mathrm{ATN})$ was also derived for aerosol particles sampled in a car-parking garage as well as at a high alpine site (Jungfraujoch). During the AIDA chamber experiments, the quantification of the shadowing effect was possible due to the large

Table 2
Determined fitting parameter f (see Eq. (8)) describing the shadowing effect for different aerosol types

Experiment/aerosol type	Aging time (h)		Spectrum Aethalometer AE30						AE10	
			450 nm	590 nm	615 nm	660 nm	880 nm	950 nm	Filament	bulb
Exp no. 2/Diesel soot	Fresh	0.5	1.60	1.66	1.65	1.64	1.65	1.61	1.50	
	Aged	42.3	1.51	1.58	1.55	1.55	1.55	1.53	1.50	
Exp no. 3/Pallas soot	Fresh	2.1	1.78	1.93	1.89	1.89	1.89	1.82	1.81	
	Aged	42.7	1.51	1.63	1.59	1.57	1.60	1.54	1.60	
Exp no. 5/external mixture of Diesel soot and $(NH_4)_2SO_4$ particles	Fresh	0.5	1.47	1.54	1.53	1.55	1.55	1.55	1.45	
	Aged	23.9	1.45	1.52	1.51	1.51	1.54	1.53	1.50	
Exp no. 6/external mixture of Diesel soot and $(NH_4)_2SO_4$ particles	Fresh	0.5	1.30	1.37	1.34	1.34	1.38	1.39	1.36	
	Aged	43.0	1.15	1.20	1.20	1.20	1.23	1.24	1.28	
Exp no. 7/internal mixture of Diesel soot and organic material	Aged	17.4	1.45	1.47	1.45	1.45	1.41	1.39	1.37	
Exp no. 9/internal mixture of Pallas soot and organic material	Fresh	0.8	1.48	1.54	1.52	1.53	1.47	1.46	1.42	
	Aged	11.1	1.51	1.58	1.55	1.55	1.54	1.48	1.48	
Parking garage									1.14	
High alpine site									1.025	

chamber volume (84 m^3), providing the constant aerosol concentration during several hours necessary to perform more than one filter change by the aethalometer. For ambient aerosols a different approach for the determination of the b_{ATN} vs. ATN dependence is needed, since there the aethalometer signal shows a high variability during the time period needed to load the filter. Similar to the method described in LaRosa et al. (2002) we used two identical aethalometers measuring simultaneously the same aerosol, but performing their filter changes at different times.

In the car-parking garage mainly emissions of gasoline passenger cars were measured during 2 days. Two AE10 instruments were operated with a time resolution of 5 min and performed a total of 23 filter changes. The average BC concentration (calculated with $\sigma_{ATN}=19\ m^2\ g^{-1}$) was 6.1 μgm^3.

The other location is the high alpine research station Jungfraujoch (3580 m a.s.l., Switzerland) where two AE10 aethalometers measured simultaneously for 2 weeks (4–19 August 1999). At this site clean continental air masses were sampled, and the average BC concentration (calculated with $\sigma_{ATN} = 9.3\ m^2\ g^{-1}$ (Lavanchy et al., 1999)) was 122 ng m^{-3}. The two AE10 instruments were operated with a time resolution of 60 min and performed a total of 18 filter changes.

For these two datasets the average fit parameter f was calculated as follows: First, for both instruments an initially constant f value is assumed, and from the measured ATN data the temporal evolution of $b_{10\%}$ is calculated for both instruments with Eqs. (3) and (8). In a next step, the temporal

evolution of the ratio Q of the two $b_{10\%}$ values ($Q = b_{10\%}^{\text{Instrument 1}}/b_{10\%}^{\text{Instrument 2}}$) is computed. If Q is calculated with no shadowing correction ($f = 1$) the shadowing effect is visible in fluctuations of the temporal evolution of Q. In order to decrease these fluctuations and to determine the "best" f value characterizing the shadowing effect, f is varied and several iterations are performed to minimize

$$\Psi = \frac{\text{Percentile}(90\%, Q) - \text{Percentile}(10\%, Q)}{\text{Median}(Q)}. \tag{9}$$

With this procedure "best" f values of 1.14 and 1.025 were deduced for the car parking garage and the high alpine site Jungfraujoch dataset, respectively, and—compared to the untreated "raw" data ($f = 1$) $-$ Ψ was lowered by 28% and 3.4%, respectively.

In the following it will be shown that the magnitude of the shadowing effect (i.e. the determined f values) is inversely proportional to the aerosol light scattering behavior. For the parameterization of this effect we use the aerosol single scattering albedo ω_0 (see Eq. (5)). A comparison of the different aerosols shows the following tendencies (see Table 2): "Pure" soot particles (Exp. 2 and 3) having a $\omega_0 < 0.3$ are characterized by a distinct decrease of b_{ATN} as a function of ATN. This is seen in high f values, with f typically $\sim$1.5 for Diesel soot particles. Palas soot particles show an even higher shadowing effect ($f = 1.5$–1.9). The detailed reasons for this difference are presently unknown but one could imagine that the smaller particle sizes of the Palas soot particles are responsible for a different (denser) incorporation of the particles in the fiber matrix resulting in a more efficient covering (increased shadowing).

Mixed aerosols (i.e. when light scattering material is added to the soot particles) are characterized by smaller f values. This smaller decline of b_{ATN} with increasing ATN is attributed to the incorporation of scattering material in the filter matrix, which partly compensates for the light absorption of soot particles. This behavior is observed for internal as well as external mixtures. It is clearly seen that the parking garage aerosol leads to a significantly smaller shadowing effect compared to the Diesel engine particles. Again, we attribute this to the incorporation of scattering (organic) material in the filter matrix since gasoline engine particles are known to be composed of a higher fraction of organic material compared to the emissions of Diesel engines (Burtscher et al., 2001). The high fraction of scattering material is also responsible for the even lower f values determined at the high alpine site where the particles are characterized with a ω_0 being typically larger than 0.7 (Collaud Coen et al., personal communication).

Fig. 4 shows the determined f values as a function of $1 - \omega_0$, where ω_0 was calculated with the reference scattering and extinction measurement. Measurements are presented for the wavelength of λ=660 nm. Despite the scatter of the data, the overall trend shows a clear dependence of f on ω_0 as well as on the aerosol type (i.e. Palas soot particles are characterized by higher shadowing than Diesel soot particles).

In order to present a correction of the shadowing effect (see Section 4.2.4), the data for "pure", internally and externally mixed Diesel soot particles was fitted with the following linear relation:

$$f = a(1 - \omega_0) + 1 \tag{10}$$

and the determined parameter a was found to be 0.87 ± 0.10 and 0.85 ± 0.05 at $\lambda = 450$ and 660 nm, respectively. The f values determined with Palas soot particles were excluded in this parameterization since these particles are not representative for atmospheric aerosols.

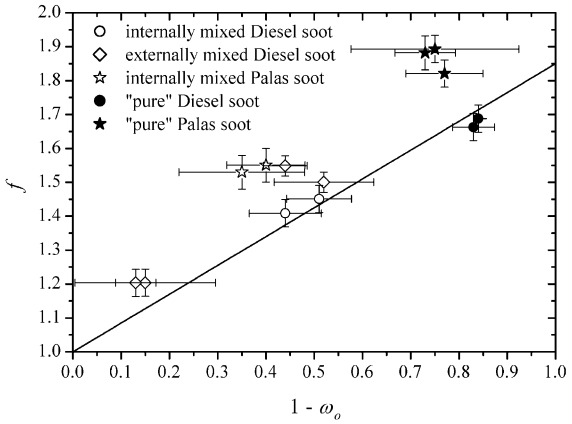

Fig. 4. Determined f values (a measure for the shadowing effect) at $\lambda = 660$ nm vs. $1 - \omega_0$ (ω_0 is the single scattering albedo for the particles in the airborne state). Different symbols are used to distinguish between different aerosols. The line is a fitted curve (Eq. (10)) which visualizes the trend for "pure" and internally mixed diesel particles and can be used for a correction of the shadowing effect.

Table 3
Determined C values describing the enhanced light absorption in the unloaded fiber filter

Wave-length λ (nm)	"Pure" Diesel soot particles	"Pure" Palas soot particles	Externally mixed Diesel and $(NH_4)_2SO_4$ particles	Internally mixed (coated) Diesel soot particles	Internally mixed (coated) Palas soot particles
450	2.08 ± 0.55	2.10 ± 0.52	2.09 ± 0.95	3.64 ± 0.98	3.35 ± 0.78
660	2.13 ± 0.57	2.23 ± 0.79	2.29 ± 1.36	3.90 ± 1.13	3.66 ± 1.53

The errors were calculated by error propagation from the uncertainties in the measurement of b_e and b_s. Note that the higher C values determined during the coating experiments are caused by a condensation artefact (see text).

4.2.2. *Parameterization of multiple scattering in the unloaded fiber filter*

In the following, we will quantify the enhanced light attenuation in the unloaded filter on an empirical basis by comparing the filter based attenuation measurements with the simultaneously measured reference values for airborne particles. For periods where b_{abs} and b_{ATN} were available, the aethalometer data were parameterized with Eq. (8), and the empirical correction factors C at $\lambda = 450$ and 660 nm were deduced according to

$$C = \frac{b_{10\%}}{b_{abs}}. \tag{11}$$

Table 3 summarizes the obtained C values for different investigated aerosol types. The averages were calculated from measurements performed at different aging times (i.e. for freshly produced as well as aged aerosols). The indicated errors of these values were calculated by error propagation from the uncertainties of b_{abs}, b_{ATN} and b_s.

Pure Palas and Diesel soot particles, as well as externally mixed Diesel soot particles, are characterized on average by $C = 2.09 \pm 0.41$ and 2.22 ± 0.56 at $\lambda = 450$ and 660 nm, respectively. During all these experiments no significant change of C was observed with aging time. The values agree

well with $C = 1.9$—the value which is often applied to AE10 aethalometers without consideration of the particles shadowing effect.

No significant changes in the C values were observed during the experiments where Diesel soot was externally mixed with $(NH_4)_2SO_4$ particles. The reason for this agreement is due to the fact the C values characterize the enhanced light scattering of nearly unloaded filters (ATN = 10%). The additional multiple scattering arising from the non-absorbing $(NH_4)_2SO_4$ particles was already accounted for in the calculation of $b_{10\%}$ by applying the determined lower f values.

Table 3 also shows that significantly higher values (on average: $C = 3.6 \pm 0.6$) were determined during the experiments where soot particles were coated with organic material. During these experiments we observed a decrease of C with aging time: At the end of the experiments ($t > 10$ h) the C values were on average about 20% lower than the ones determined just after onset of the coating ($t \sim 1$ h). The higher C values are attributed to a condensation artefact which is more pronounced at the beginning of the coating experiments where high concentrations of semi-volatile oxidation products (such as pinonaldehyde) were formed by the ozonolysis of α-pinene. This artefact originates from these gaseous species that condense on the "fresh" aethalometer filter in the first few minutes after every filter change. After this time period the filter is saturated and in equilibrium with the gas phase. The additional scattering material adsorbs on the filter fibers and leads to a significant increase of the optical path in the filter, which explains the observed positive artefact in the b_{ATN} measurement. Such condensation processes are confirmed by Saathoff et al. (2003c) who showed that during these experiments vapor phase organics adsorbed on quartz fiber filters resulting in an additional apparent total carbon increase of $\sim 45\ \mu g\ m^{-3}$ which is similar to the mass concentration of the freshly produced secondary organic aerosol particles. Such high concentrations of condensable species are not present in the remote atmosphere, and therefore the higher C values determined during these experiments are believed not to apply to aged atmospheric aerosols. However, care has to be taken when aethalometer measurements are performed close to combustion sources (as in test bench studies) where relatively high concentrations of semi-volatile species are present. Thus, more research is needed in this respect.

4.2.3. Wavelength dependence

The spectrum aethalometer allows for the determination of the attenuation coefficient over a wide spectral range ($\lambda = 450$–950 nm). For the different aerosol types, Figs. 5a–e show the wavelength dependent comparison of the reference absorption coefficient with the absorption coefficient calculated from the filter based attenuation measurement. Here, the aethalometer data was corrected for (i) the shadowing effect (by applying the appropriate f values from Table 1) and (ii) the multiple scattering in the fiber matrix (by using a constant C value of 2.09 as determined for externally mixed particles at $\lambda = 450$ nm). The AE10 data was also corrected in the same manner and is also included in the figures at $\lambda = 840$ nm. The broadband spectral sensitivity of this instrument is reflected in large horizontal error bars. The vertical error bars reflect the experimental uncertainties and were calculated by error propagation. The solid lines in the figures serve as guides to the eye and were obtained by fitting the reference b_{abs} data with an empirical Ångström power law (see Schnaiter et al., 2003 for more details). In Figs. 5a and b the different Ångström exponents determined for "pure" Diesel and Palas soot particles were applied. For mixed aerosols (Figs. 5c–e) the exponent of the corresponding "pure" soot type (Diesel or Palas) was used.

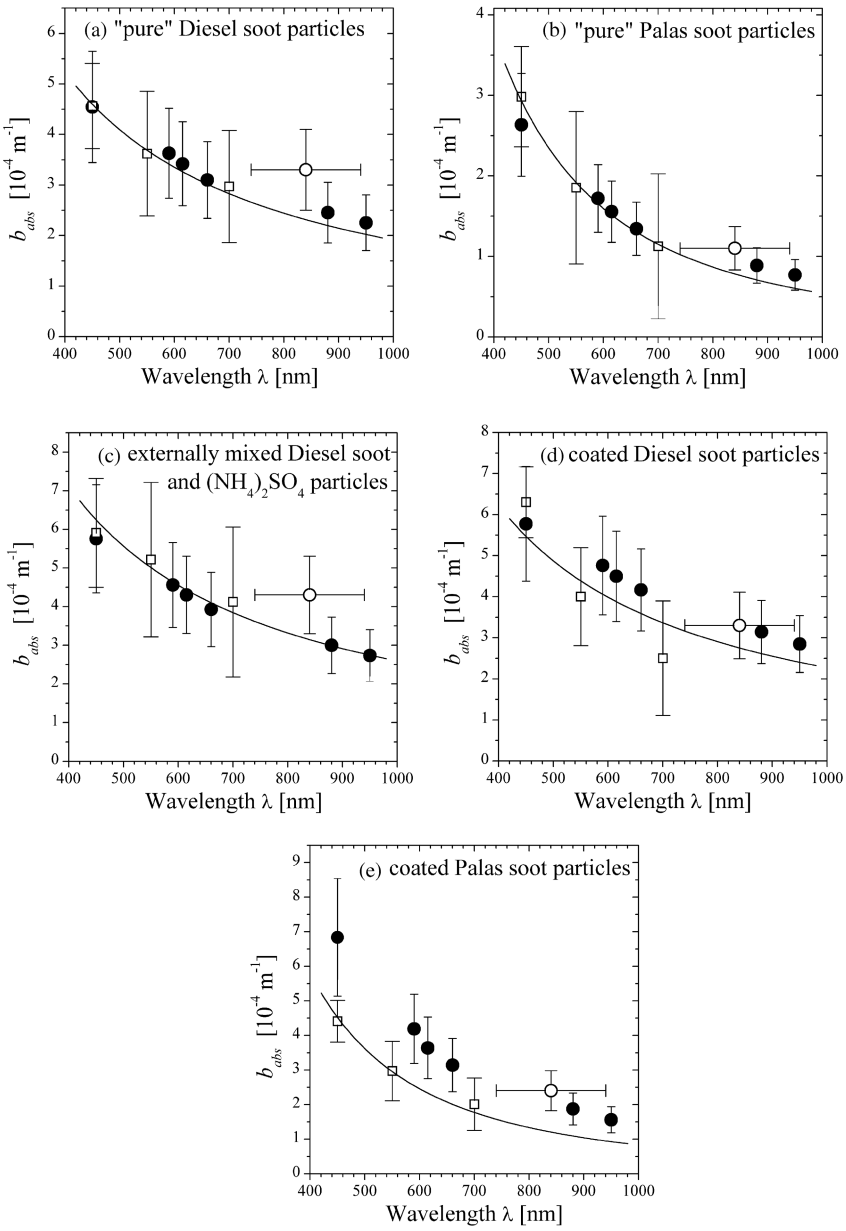

Fig. 5. Wavelength dependent comparison of the measured absorption coefficient of the spectrum aethalometer (AE30, solid circles), of the conventional aethalometer (AE1O, open circle) as well as the reference absorption coefficients for airborne particles (open squares) for different aerosols. The aethalometer data was corrected for the shadowing effect as well as for multiple scattering in the filter matrix by applying a constant C value of 2.09 that was determined for uncoated particles (see text). The solid lines are guides to the eye and were obtained by fitting the reference b_{abs} data with an Ångström power law $b_{abs} \propto \lambda^{-\alpha}$. The Ångström exponents α are taken from Schnaiter et al. (2003) and are 2.1 and 1.1 for Palas and Diesel soot, respectively.

A good agreement is found between the corrected spectrum aethalometer data and the reference absorption coefficient for uncoated soot particles (Figs. 5a–c). Due to the condensation artefact, this instrument overestimates b_{abs} for coated soot particles (Figs. 5d and e). This is not surprising since $C = 2.09$ applies only to the uncoated soot particles (see Table 3). However, within the experimental uncertainty, the overall wavelength dependence of b_{abs} is well reflected by the spectrum aethalometer, which is a strong indication that C experiences no significant wavelength dependence. This justifies the use of a constant C value over the wider spectral range. It is also seen that the AE10 instrument predominately overestimates b_{abs} by about 10–40%. Whether this is due to the ill-defined instrumental spectral sensitivity of the AE10 aethalometer or due to the different filter material employed in the two aethalometers remains an open question.

4.2.4. Aethalometer correction

The goal of this paper is to present correction factors for the use of the aethalometer. The whole correction procedure is based on the idea to convert all b_{ATN} values to $b_{10\%}$, which then can be converted into b_{abs} values using the calibration factor C. For this purpose, intermittent attenuation measurements at low filter loadings (ATN$\sim$10%) are first extracted from the given aethalometer raw dataset. These values are not affected by the shadowing effect. Using Eq. (9), they can thus be used to calculate intermittent b_{abs} values. These individual measurements are averaged over the time of interest and yield an estimate of the mean b_{abs}. From this value, the average ω_0 of the aerosol is calculated using concurrent nephelometer measurements (b_s). Then, an average f value is deduced with Eq. (10). Using Eq. (8), this value is then applied to the whole data set to convert all b_{ATN} values to $b_{10\%}$. The values can then be converted into "final" b_{abs} values using Eq. (11).

5. Summary

In this work the response of two different aethalometers (AE10 and AE30) to several types of soot was investigated. We have shown that the determination of the light absorption coefficient (b_{abs}) with the AE10 aethalometer is a difficult task because of an ill-defined spectral sensitivity of this instrument. The spectrum aethalometer (AE31 as well as the commercial AE31) on the other hand allows for the measurement of b_{abs} over a wide spectral range, provided that the proper numerical corrections are performed.

During all experiments it was found that with increasing aethalometer filter load the optical path in the filter decreased. As a result, an increasing underestimation of the measured aethalometer raw signals (such as absorption coefficient or black carbon mass concentrations) occurs with increasing filter loads. This is attributed to a shadowing effect and is caused by a reduction of multiple light scattering in the filter by the embedded light absorbing particles. This artefact is very distinct for "pure" soot particles where a filter change causes an apparent increase of the measured signals by a factor of about 1.6. This is in contrast to the behavior determined in clean continental air at the high alpine site Jungfraujoch. There, a filter change causes an apparent signal increase of only about 3% and it is therefore concluded that the shadowing effect is almost negligible for aged atmospheric aerosols. This difference at the remote site is explained by the incorporation of a high amount of scattering aerosol material in the fiber matrix, which partially compensates the shadowing effect. It was found that the magnitude of this effect (f value) is linearly related to the single scattering

albedo ω_0 of the sampled aerosol. Thus knowledge of the aerosol light scattering behavior is needed for the correction of aethalometer data.

Another instrumental artefact is the enhanced light absorption of the filtered particles caused by multiple scattering of the light beam at the filter fibers (C factor). A comparison with the reference method at $\lambda = 450$ and 660 nm showed that "pure" Palas and Diesel soot particles experience an average enhanced absorption of $C = 2.14 \pm 0.21$ in the filter. This value applies also for mixed Diesel soot and $(NH_4)_2SO_4$ particles because this C value characterizes the enhanced light scattering within the nearly unloaded filters. A significantly higher C value (3.6 ± 0.6) was determined during experiments where soot particles were coated with oxidation products of α-pinene. This higher value is attributed to the experimental conditions where high concentrations of semi-volatile gaseous species adsorbed on the aethalometer filter fibers and thus enhanced multiple light scattering. Therefore, denuders are required in front of the aethalometer in cases where an aerosol with relatively high concentrations of condensable gaseous species is sampled.

If filter based absorption measurements are not corrected for these artifacts, the derived absorption coefficients will be too high, meaning that climate relevant parameters such as the single scattering albedo are underestimated. The corrections presented in this paper will enhance the accuracy of long-term aethalometer datasets. However, one has to mention that the C factors were determined in AIDA aerosol chamber experiments and have not yet been demonstrated to apply also to aged atmospheric aerosols. This verification should have a high priority in future research in this area.

Acknowledgements

Christoph Hüglin (EMPA) provided the AE10 instrument for this study. This work was supported by the Global Atmosphere Watch (GAW) programme of the World Meteorological Organization. We thank the referees for their helpful comments.

References

Ballach, J., Hitzenberger, R., Schultz, E., & Jaeschke, W. (2001). Development of an improved optical transmission technique for black carbon (BC) analysis. *Atmospheric Environment*, *35*(12), 2089–2100.

Bodhaine, B. A. (1995). Aerosol absorption measurements at Barrow, Mauna Loa and the south pole. *Journal of Geophysical Research*, *100*(D5), 8967–8975.

Bond, T. C., Anderson, T. L., & Campbell, D. (1999). Calibration and intercomparison of filter-based measurements of visible light absorption by aerosols. *Aerosol Science and Technology*, *30*(6), 582–600.

Burtscher, H., Baltensperger, U., Bukowiecki, N., Cohn, P., Hüglin, C., Mohr, M., Matter, U., Nyeki, S., Schmatloch, V., Streit, N., & Weingartner, E. (2001). Separation of volatile and non-volatile aerosol fractions by thermodesorption: Instrumental development and applications. *Journal of Aerosol Science*, *32*(4), 427–442.

Gundel, L. A., Dod, R. L., Rosen, H., & Novakov, T. (1984). The relationship between optical attenuation and black carbon concentration for ambient and source particles. *The Science of the Total Environment*, *36*, 197–202.

Hansen, A. D. A., Rosen, H., & Novakov, T. (1984). The aethalometer—an instrument for the real-time measurement of optical absorption by aerosol particles. *The Science of the Total Environment*, *36*, 191–196.

LaRosa, L. B., Buckley, T. J., & Wallace, L. A. (2002). Real-time indoor and outdoor measurements of black carbon in an occupied house: An examination of sources. *Journal of the Air and Waste Management Association*, *52*(1), 41–49.

Lavanchy, V. M. H., Gäggeler, H. W., Nyeki, S., & Baltensperger, U. (1999). Elemental carbon (EC) and black carbon (BC) measurements with a thermal method and an aethalometer at the high-alpine research station Jungfraujoch. *Atmospheric Environment*, *33*(17), 2759–2769.

Lindberg, J. D., Douglass, R. E., & Garvey, D. M. (1993). Carbon and the optical-properties of atmospheric dust. *Applied Optics*, *32*(30), 6077–6081.

Lindberg, J. D., Douglass, R. E., & Garvey, D. M. (1999). Atmospheric particulate absorption and black carbon measurement. *Applied Optics*, *38*(12), 2369–2376.

Liousse, C., Cachier, H., & Jennings, S. G. (1993). Optical and thermal measurements of black carbon aerosol content in different environments: Variation of the specific attenuation cross-section, sigma. *Atmospheric Environment*, *27A*(7), 1203–1211.

Penaloza, M. A. (2000). An alternative method of studying the optical properties of highly non-absorbing spherical monodisperse aerosol using a cell transmissometer. *Journal of Aerosol Science*, *31*(10), 1231–1250.

Petzold, A., Kopp, C., & Niessner, R. (1997). The dependence of the specific attenuation cross-section on black carbon mass fraction and particle size. *Atmospheric Environment*, *31*(5), 661–672.

Petzold, A., & Niessner, R. (1995). Method comparison study on soot-selective techniques. *Mikrochimica Acta*, *117*, 215–237.

Reid, J. S., Hobbs, P. V., Liousse, C., Martins, J. V., Weiss, R. E., & Eck, T. F. (1998). Comparisons of techniques for measuring shortwave absorption and black carbon content of aerosols from biomass burning in Brazil. *Journal of Geophysical Research Atmospheres*, *103*(D24), 32031–32040.

Saathoff, H., Möhler, O., Schurath, U., Kamm, S., Dippel, B., & D., M. (2003a). The AIDA soot aerosol characterisation campaign 1999. *Journal of Aerosol Science*, *34*, 1277–1296.

Saathoff, H., Naumann, K.-H., Schnaiter, M., Schöck, W., Möhler, O., Schurath, U., Weingartner, E., Gysel, M., & Baltensperger, U. (2003b). Coating of soot and $(NH_4)_2SO_4$ particles by ozonolysis products of α-pinene. *Journal of Aerosol Science*, *34*, 1297–1321.

Saathoff, H., Naumann, K.-H., Schnaiter, M., Schöck, W., Weingartner, E., Baltensperger, U., Krämer, L., Bozoki, Z., Pöschl, U., Niessner, R., & Schurath, U. (2003c). Carbon mass determinations during the AIDA soot aerosol campaign 1999. *Journal of Aerosol Science*, *34*, 1399–1420.

Schmid, H., Laskus, L., Abraham, H. J., Baltensperger, U., Lavanchy, V., Bizjak, M., Burba, P., Cachier, H., Crow, D., Chow, J., Gnauk, T., Even, A., ten Brink, H. M., Giesen, K. P., Hitzenberger, R., Hueglin, C., Maenhaut, W., Pio, C., Carvalho, A., Putaud, J. P., Toom-Sauntry, D., & Puxbaum, H. (2001). Results of the carbon conference international aerosol carbon round robin test stage I. *Atmospheric Environment*, *35*(12), 2111–2121.

Schnaiter, M., Horvath, H., Möhler, O., Naumann, K.-H., Saathoff, H., & Schöck, O.W. (2003). UV-VIS-NIR spectral optical properties of soot and soot-containing aerosols. *Journal of Aerosol Science*, *34*, 1421–1444.